Available online at www.sciencedirect.com

ScienceDirect

Procedia Engineering 205 (2017) 3285–3292

Procedia Engineering

www.elsevier.com/locate/procedia

10th International Symposium on Heating, Ventilation and Air Conditioning, ISHVAC2017, 19-22 October 2017, Jinan, China

# A Study of Particle Deposition in Ventilation Ducts With Convex or Con-cave Wall Cavity

Feifei Wang*, Enshi Zhang, Jinbo Wang

*School of environment science&enginering, Huazhong University of Science & Technology, Wuhan, China, 430074*

**Abstract**

This article numerically investigates particle deposition in the ventilation ducts with convex or concave wall cavity. The utilized models can accurately reproduce the related data in the previous studies. Characteristics of the airflow and particles tracks are also investigated. Compared with that in the smooth duct, the particle deposition velocity increases greatly in the ducts with various wall cavities. Mechanisms of the enhancement of particle deposition are further analyzed. The interception by the cavities, the expanded deposition area, and the enhanced flow turbulence are conducive to the particle deposition. Ventilation ducts with convex/concave wall cavity can be considered as an efficient method to reduce PM2.5. In addition, $V_d^+$ increases more quickly in the duct with the convex cavity than that with the concave cavity.


Peer-review under responsibility of the scientific committee of the 10th International Symposium on Heating, Ventilation and Air Conditioning.

*Keywords:* Numerical simulation; Ventilation duct; Particle deposition; Deposition velocity

## 1. Introduction

Fine/micro particle matter (PM) exposure is becoming an essential incentive to the human health [1]. Reduction of PM, either in the atmospheric or in the indoor air, has attracted great interests of scientists and engineers over the world. Ventilation ducts in the air-conditioning system are the main connection of indoor and outdoor environment. Though typically equipped with various filters to percolate the airborne particles, the airflow inside the ventilation ducts can still carry a large quantity of particles into the indoor. On the other hand, when the airborne particles travel through the ventilation ducts, they are affected greatly by different forces and might deposit on the wall surfaces. It is

*Corresponding author. Tel.: +86-13294160016
*E-mail address: ffwang@hust.edu.cn*

1877-7058 © 2017 The Authors. Published by Elsevier Ltd.
Peer-review under responsibility of the scientific committee of the 10th International Symposium on Heating, Ventilation and Air Conditioning.
10.1016/j.proeng.2017.10.336

hence important to investigate the particle characteristics in the ventilation ducts for the controlling of the indoor airborne PM level.

To explore effective methods to reduce PM, a large quantity of research on the particle depositions is carried out, generally via experiments or modeling. On the experimental side, they are implemented and can provide valuable and accurate data, such as those reviewed by Lai [2] and recently by Bouilly et al. [3]. However, in a practical ventilation system, inside airflow is typically turbulent and the airborne particles move randomly. As a result, though the relationships between the particle deposition velocity and the particle sizes from various experiments exhibit a similar trend, those measured data can differ significantly by one to two orders of magnitude [4]. In particular, it is very difficult to measure all the crucial information. Thus, the experimental investigation of the particle behavior in the ventilation duct is quite challenging.

Computational fluid dynamics (CFD) modeling is another important way to study particle characteristics in ventilation ducts [5]. Modeling work is mainly focused on either replicating the measurements or understanding the physical observations. Zhang and Chen [6] and Gao et al. [7] investigated the accuracy and capability of various turbulent models, i.e., $v^2$-$f$ model, Reynolds stress model (RSM), RNG $k$-$\varepsilon$ model and SST $k$-$\omega$ model, coupled with some proper corrections to the near-wall turbulence. They found that all of those RANS turbulent models coupled with some adequate corrections to the flow field can successfully predict the particle deposition velocity in ventilation ducts. On the other hand, many studies were carried out for the application of CFD models to predict particle deposition in ventilation ducts with various forms [9 ~13]. Lacono et al. [8] numerically found that the surface ribs on the wall could intercept particles and accelerate the accumulation. Lu and Lu successfully built an accurate numerical model to predict the particle behavior in ventilation ducts with ribs. It was found the surface ribs may significantly strength the particle deposition which is consistent with the experimental observation. Their studies also investigated the effect on the enhancement efficiency of the rib parameters, e.g., shape, arrangement configuration, spacing, and height.

The above discussion show that the roughness of wall surface has great impacts on the deposition of the airborne particles. The indoor air quality (IAQ) can be obviously improved if particles can be intercepted and deposit on the wall surface of the ventilation systems. Most previous studies carried out the investigation of particle deposition in ventilation duct with ribs. In this study, ventilation ducts with convex and concave wall cavity is concerned, and the numerical investigation of the aerodynamics characteristics and deposition of the airborne particles in the duct is presented. The enhancement efficiency and mechanisms of the particle deposition in the ducts with convex and concave wall cavity are seriously studied and discussed.

## 2. Model descriptions

The schematic diagrams of the investigated smooth duct, duct with convex wall cavity, and duct with concave wall cavity are shown in Figure 1. The smooth duct as shown in Figs. 1(a) is studied here for validation of the numerical models, and also is used as a reference for the other two ducts. The lengths and heights of all three ventilation ducts are 400 and 20mm, which are the same as that used in the literatures [9~13]. To ensure the airflow in the ducts is fully developed into turbulent state, the first halves of all ducts are smooth ($x$ < 200 mm). For the latter half, nineteen pairs of convex and concave cavities are arranged on the two sides of these two ducts separately as shown in Figs. 1(b) and (c). The convex wall cavity has the same size as the concave one but in the opposite direction. The length and height of the cavities are all 1mm, and the distance between each other is 10 mm.

For all the calculations, the velocity and the density of the airflow are fixed at 5.5 m/s and 1.225 kg/m$^3$ at 288 K. The Reynolds number can be calculated as 7532. 30,000 spherical solid particles at the same diameter are released into the airflow at $x$ = 200 mm, which is selected as the particle release position to ensure the flow field is fully developed. The density of the particle is 2000 times the density of air. In this study, the heat exchange among the particles, air and the wall is not ignored. The velocity and the temperature of the particle is the same as that of the airflow. Several different diameters of the particles, i.e., 0.1, 0.2, 0.3, 0.5, 1, 2, 3, 5, 10, 20, 30 and 50 $\mu m$, are investigated in this study.

In numerical studies, the fluid flow field is described by Navier-Stokes equations, including the conservations of continuity, momentum, and energy, etc. RSM model with a near-wall correction to the normal turbulent fluctuating velocity is utilized to predict the turbulent air-flow field. A two-layer zonal model with enhanced wall function is selected to predict the turbulent flow in the near wall region. More details about the RSM model are referred in the literature [14].

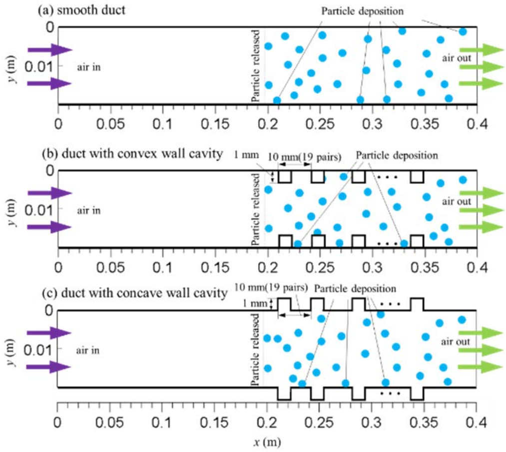


Fig. 1. Schematic diagrams of the investigated ventilation ducts

This study used Lagrangian method to predict particle deposition. Because the concentration of the airborne particle is quite low, the impact of the particles on the flow and the collision between particles are ignored. Discrete random walk (DRW) model is implemented to predict the particle movement caused by the turbulent dispersion. To obtain a more accurate flow field, this study implements some corrections by adopting curve-fitted values of fluctuating velocity in the wall-normal direction. For all cases, the corrections are as Eq.(1) [15].

$$v^+_{rms} = \frac{v'_{rms}}{u^*} = \frac{a(y^+)^2}{1+by^+c(y^+)^2} \text{ at } y^+ < 30 \tag{1}$$

$$u^* = \sqrt{\frac{\tau_w}{\rho}} = U_{mean}\sqrt{f/2} \tag{2}$$

where the constant $C$, $a$, $b$ and $c$ are 0.008, 0.0116, 0.203, and 2.421 respectively, $y^+$ ($\equiv yu^*/v$) is the normalized wall distance, and $u^*$ is the friction velocity. $\tau_w$ is the wall shear stress $(1/2\rho U^2_{mean}f)$, $u_{mean}$ is the mean velocity of the air and $f$ is the friction factor as expressed as $f = 0.0791.Re^{-0.25}$.

The three ducts as shown in Figure 1 are all considered as two-dimensional, and all of them are discretized to orthogonally structured meshes. After verifying the grid-independency, the meshes with 32000, 69180, and 67960 grids are respectively used for the smooth duct, the ducts with convex and concave wall cavities. The non-slip velocity wall condition is implemented to the wall. Because of their small diameters, the particles are assumed to be trapped once they contact with the wall and no reflection and collision between them are considered. To obtain an accurate flow field, the one-seventh power law is employed to express the velocity, the turbulent kinetic energy ($k$) and its dispersion ($\varepsilon$) at inlet.

All the transport equations (continuity, momentum, turbulence kinetic energy, RSM, $\varepsilon$, and DPM) are solved using the commercial package ANSYS FLUENT v14.0 [14]. The SIMPLE algorithm method is utilized to solve pressure and velocity coupling. The POSI scheme is selected to solve the pressure equation. The Runge-Kutta method and the DRM model are used to track the path of the particles. The second-order upwind scheme is employed for discretizing the equations in order to improve the accuracy of the simulations. To improve the prediction of the flow field, UDFs (user defined function) are used to introduce the boundary condition of the velocity distribution at inlet. Solution convergence is determined by two criteria. The first one is to ensure that the numerical residuals are $<10^{-6}$ for all the variables. The second criterion is to ensure that the variations between consecutive iterations of velocity are kept within 0.1 m/s at the downstream outlet of the computational domain. After the convergence of the flow field, a UDF, .i.e., Eq. (4), is used to modify the instantaneous fluctuating velocity near the wall region in the ventilation duct.

## 3. Validation of the numerical models

To validate the present models, the prediction of the turbulent flow in the horizontal smooth ventilation duct was first carried out. Figure 2 shows the non-dimensional mean velocity ($u^+ = u/y^+$) and the turbulent fluctuating wall-normal velocity ($v^+_{rms}$) against $y^+$ at $x$ = 300 mm. In this figure, the results with or without the modification of Eq. (14) are presented. The direct numerical simulation (DNS) data of Kim et al. [13] is also included for comparison.

Figure 2(a) shows that the present models can well reproduce the DNS data. Since Eq. (1) is only used to modify the $v^+_{rms}$, it has little effect on the mean air velocity. Figure 2(b) illustrates that the use of Eq. (1) is critical to correctly predict the distribution of $v^+_{rms}$, especially in the near-wall region. For $y^+ < 30$, the models without correction overestimates $v^+_{rms}$ while the predictions match the DNS data well with the correction of Eq.(1). For $y^+ > 30$, the numerical models with and without correction respectively produce similar results, i.e. slight underestimations of the DNS data. That is, the flow field may approximately capture the features of the airflow process.

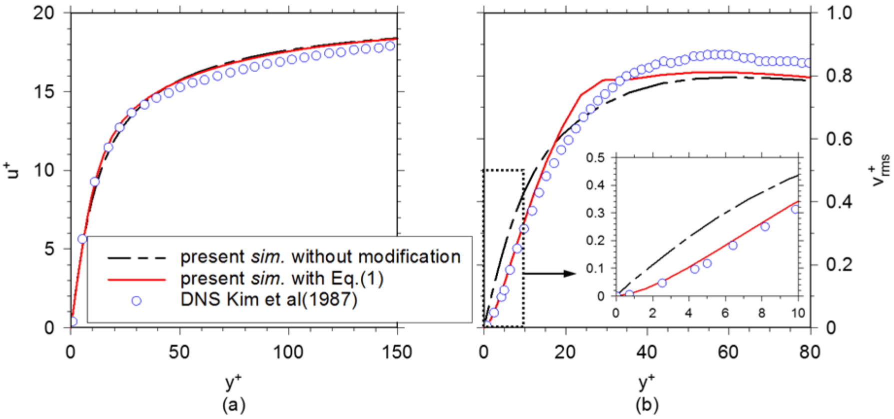


Fig. 2. (a) non-dimensional mean velocity ($u^+$) ; (b) turbulent fluctuating velocity ($V^+_{rms}$) *versus* the wall $y^+$ in the horizontal smooth ventilation duct

The strength of particle deposition is usually characterized by its velocity as Eq.(3). The total of the particles deposited per unit time on the unit area of the duct is as Eq.(4). The relationship between the dimensionless deposition velocity ($V_d^+$) and the relaxation time ($\tau^+$) of the particle is usually employed to evaluate the particle deposition efficiency (Zhang and Chen 2007). The dimensionless deposition velocity ($V_d^+$) is as Eq. (5). The relaxation time ($\tau^+$) of the particle is a function of the particle diameter ($d_p$) Eq.(6).

$$V_{\mathrm{d}} = J/C_0 \tag{3}$$

$$J = N_{\mathrm{d}}/t/A \tag{4}$$

$$V_d^+ = V_d/u^* \tag{5}$$

$$\tau^+ = C_c S d_p^2 u^{*2}/18v^2 \tag{6}$$

where, i.e., where $J$ is, i.e., and $C_0$ is the average particle concentration in the air-flow, i.e., $C_0 = N_0/V$. Here, $N_{\mathrm{d}}$, $N_0$, $t$, $A$, and $V$ are, respectively, the number of the particles deposited onto the wall surface, the total number of particles initially released into the air-flow, the residence time of one particle in the duct, the cross-section area and volume of the duct.

Figure 3 plots $V_d^+$ against $\tau^+$ for the particle deposition in the smooth duct. For comparison, the experimental results, the empirical formula fitting curve, and the numerical results from other researchers [9 ~ 13] are also presented. Because of the random motion of the particles in the duct, the particle deposition efficiency (i.e., the relationships between $V_d^+$ and $\tau^+$) from various work cannot always matches one curve. However, it is obvious that $V_d^+$ in the duct presents a clear *S*-shape trend with the increase of $\tau^+$. The results show the predicted particle deposition by used the present models in this study is basically consistent with the previous data. The comparisons in Figs. 3 and 4 shows that the models and methods presented in this paper can accurately predict the particle motion and the flow characteristics in the smooth ventilation duct. Therefore, the same models is appropriate to predict the particle deposition in the ventilation ducts with convex and concave wall cavities respectively.

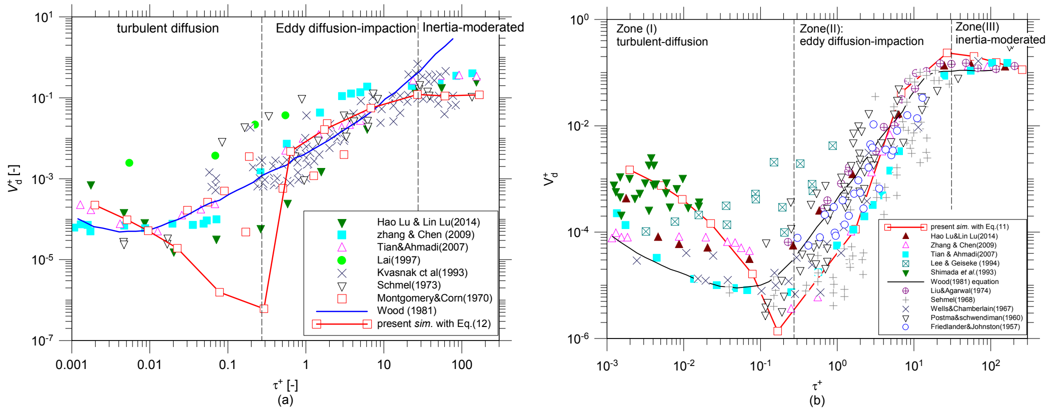


Fig. 3. (a)Comparison of the particle deposition velocity $V_d^+$ in the horizontal (a); vertical (b) ducts with smooth wall.

## 4. Results and analysis

As presented before, the prediction of airflow characteristic and particle deposition in the smooth duct by using the models with correction were validated by using the published literatures. These models are further used to predict the airflow characteristic and particle deposition etc. in the ducts with convex and concave wall cavities respectively.

### *4.1 Particle deposition enhancement*

Figure 4 presents the particle deposition velocity ($V_d^+$) and its enhancement ratio in the ventilation ducts with and without wall cavities verse $\tau^+$. The enhancement ratio of $V_d^+$ is the increasing rate with respect to that in the smooth duct. Figure 4 (a) shows the particle deposition is significantly enhanced as a whole with the help of the convex or concave wall cavity when compared with the results from the smooth duct. The particle deposition in the duct with the convex wall cavity appears to be higher by about one order of magnitude than that with the concave wall cavity for $\tau^+ < 20$. For $\tau^+ > 100$, the particle deposition are almost the same. This figure also shows that $V_d^+$ exhibits a weakened $S$-shape trend with the increase of $\tau^+$ and the growth of $V_d^+$ slows down in the eddy diffusion-impaction and inertia-moderated regimes.

Figure 4(b) indicates that the enhancement ratio changes greatly as $\tau^+$ varies. For finer particles, the enhancement ratio increases with $\tau^+$. In other words, for $\tau^+ < 0.3$, the particle deposition is strengthened by about 2-4 orders of magnitude, and it increases until an peak value, i.e., 7770 times and 1320 times respectively for the ducts with the convex and concave wall cavities respectively at $\tau^+ \approx 0.3$. In contrast, in the eddy diffusion-impaction regime and the inertia-moderated regime, the minimum enhancement ratio are only 1.3 and 1.1.

Nevertheless, Figure 4 reveals that both the convex and concave wall cavities have great effect on the particle deposition in ventilation ducts. Furthermore, this effect becomes more efficient for the particles with small sizes. Therefore, implementation of convex or concave wall cavity in ventilation ducts may provide an effective method for removing fine particle matters, e.g., PM2.5.

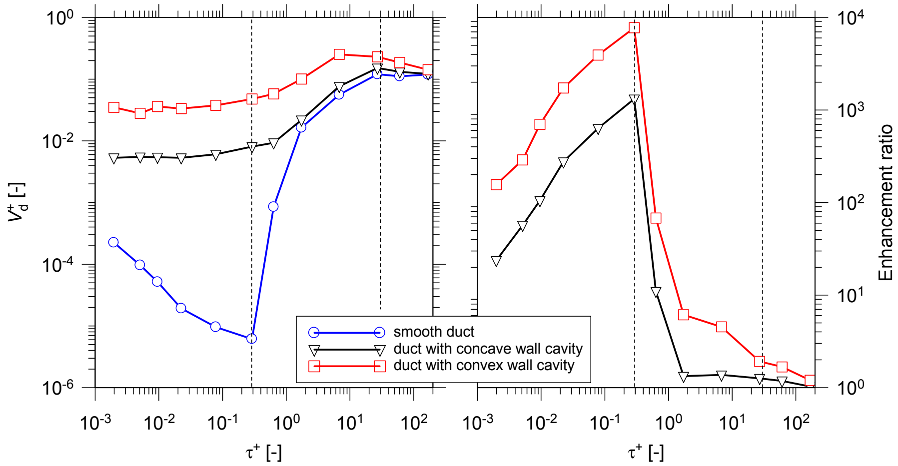


Fig. 4. (a) Particle deposition velocity $V_d^+$ (a) and its enhancement ratio (b) as a function of $\tau^+$ in the ventilation ducts with different wall

## *4.2 Mechanism of the particle deposition enhancement*

The mechanism of particle deposition enhancement in the ducts with different wall cavities is seriously analyzed. As far as the physical process is concerned, the particles in airflow can strike more easily onto the windward side of the wall surface due to the blocking effect when the convex wall cavity is implemented. In addition, the convex cavity in the duct can reduce the deposition distance of the particles to the wall. Moreover, the surface area of the ducts with cavities for particle deposition is 0.476m$^2$, which is 19% larger than 0.4m$^2$ for the smooth one as shown in Figure 1. These factors are all benefit for enhancing particle deposition.

Besides the above physical reason, particle deposition in airflow is also closely related to flow field. The structures in the first halve of the ducts are all the same, and the airflow is fully developed into the turbulent state. However, the air velocity distributions in the latter halves of these three different ducts are quite different as shown in Figure 5. Figure 5(b) indicates the air velocity is speeded up slightly for the duct with the convex wall cavity. Due to the compression effects of the convex ribs, the boundary layer deviates from the wall for some distance, and the flow in it changes greatly. Figure 6 presents these deviations in more details. Figure 5(c) shows the air velocity distribution appears to be almost the same with that in the smooth duct. This is why the pressure loss of the airflow in the duct with the concave wall cavity does not increase much.

Figure 6 shows the distribution of turbulence kinetic energy, i.e., TKE, and the flow streamlines in the smooth duct and the ducts with convex and concave wall cavities. The streamlines of the airflow in the smooth duct is nearly parallel to *x*-direction. Apparently, there is no wall-normal velocity, which is negative to the particle deposition. In contrast, Figure 6(b) and 6(c) illustrate that the streamlines are changed greatly and eddies are formed in the near-wall region of the ducts with wall cavities. That means some wall-normal velocities exist in both non-smooth ducts, which surely help to entrain particles and transport them to the wall.

On the other hand, Figure 6 also indicates that the near-wall TKE is increased greatly with the addition of wall cavities. The improved TKE can accelerate the turbulent fluctuating wall-normal velocity, which enhances the momentum exchange between the flow in the near-wall region and that in the outer. For the smooth duct, the peak TKE is only about 0.18 m$^2$/s$^2$. However, for the duct with convex wall cavity and the duct with concave wall cavity, the value becomes 2.98 and 0.6 m$^2$/s$^2$ respectively. The near-wall TKE and the turbulence intensity of the air-flow in the duct with convex wall cavity are much stronger than those in the duct with concave wall cavity as shown in Figure 6(b) and 6(c). In the duct with convex wall cavity, due to the inverse flow, there are two eddies in the space between two cavities, i.e., a larger one and relatively smaller one respectively attached at both sides of the wall cavity. Obviously, this is beneficial to the entrainment and capture of particles to the near-wall region. However, for the duct with concave wall cavity, only a small eddy can be found inside the concave cavity.

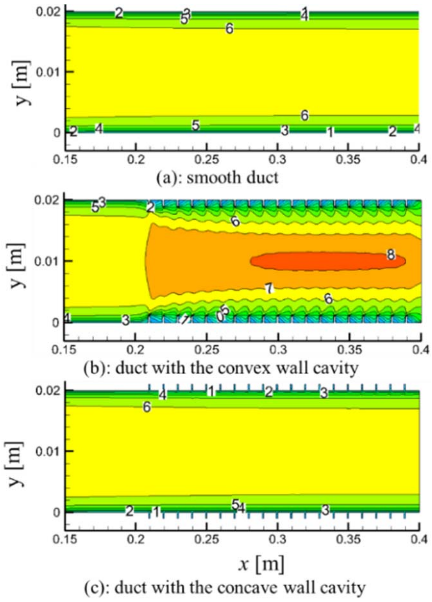


Fig. 5. Air-flow velocity distribution in the different ducts

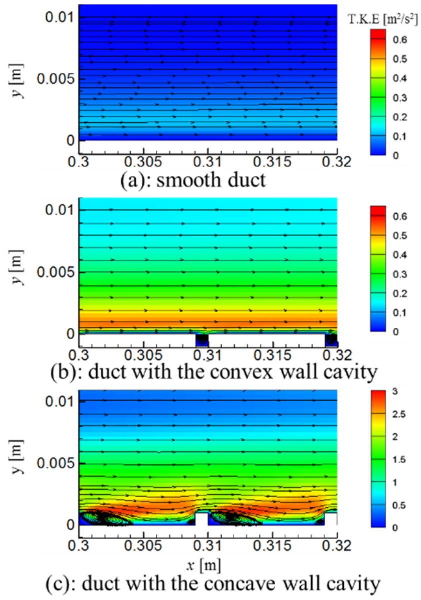


Fig. 6. TKE distribution and streamlines of air-flow in the different ducts

The strengthened turbulent fluctuation and the momentum exchange are both favorable for the airflow to entrain floating particles into eddies near the wall cavities. It is obvious that a larger TKE is conducive to particle deposition. Based on the above analysis, it can be concluded that interception by rids, expanded deposition area, and enhanced flow turbulence are all conducive to particle deposition in ducts with wall cavities. Considering the peculiar interception effect, it is obvious that the duct with the convex wall cavity results in a larger particle velocity and better particle deposition than that with the concave wall cavity as shown in Figure 4.

## CONCLUSIONS

A numerical investigation is performed on particle deposition in ventilation ducts with either convex or concave wall cavity with particle diameter ranging from 0.1μm to 50μm. The selected numerical model, i.e., RSM and DPM model with some UDF corrections, are validated by published data from previous studies. The validated models are then used to predict the performance of the ducts with different wall cavities. The conclusions may be summarized as follows: (1) the particle deposition velocity ($V_d^+$) increases greatly for the ducts with wall cavities when it is compared with that in the smooth duct. Specially, for $\tau^+ < 1$, $V_d^+$ increases by about 2~4 orders of magnitude with the peak values being 7770 and 1320 times in both ducts with convex and concave cavities respectively. For $\tau^+ > 1$, $V_d^+$ does not increase too much since the particle movement is mainly controlled by gravity and inertia; (2) $V_d^+$ increases more quickly and is higher in the duct with the convex wall cavity. This is because that the airflow structure is more complex and the turbulent kinetic energy is higher in the near-wall region of the duct with convex wall cavity than those in the duct with concave wall cavity; (3) the interception by the cavities, the expanded deposition area, and the enhanced flow turbulence are conducive to the particle deposition; (4) the addition of wall cavities can strengthen particle deposition while the duct with convex wall cavity may be much better for deposition for smaller particles. It may be an alternative for reducing PM2.5.

## Acknowledgements

The authors acknowledge the support of the National Natural Science Foundation of China (No. 51506069) and the Fundamental Research Funds for the Central Universities (HUST2016YXMS286, HUST2015061).

## References

[1] C.A. Pope, R.T. Burnett, M.J. Thun, E.E. Calle, Krewski, D., Ito, K., Thurston, G.D. Lung cancer, cardiopulmonary mortality, and long-term exposure to fine particulate air pollution. J. American Medical Association. 287 (2002) 1132-1141.
[2] A.C.K. Lai, Particle deposition indoors: a review. Indoor Air. 12 (2002) 211-214.
[3] J. Bouilly, K.Limam, D. Beghein, F. Allard, Effect of ventilation strategies on particle decay rates indoors: an experimental and modelling study. Atmos. Environ. 39 (2005) 4885-4892.
[4]A.C.K. Lai, M.A. Byrne, A.J.H. Goddard, Measured deposition of aerosol particles on a two-dimensional ribbed surface in a turbulent duct flow. J. Aerosol. Sci. 30 (1999) 1201-1214.
[5] H. Zhang, A. Goodarzl, Aerosol particle transport and deposition in vertical and horizontal turbulent duct flows. J. Fluid Mech. 406 (2000) 55-80.
[6] Z. Zhang, Q. Chen, Prediction of particle deposition onto indoor surfaces by CFD with a modified Lagrangian method. Atmos. Environ. 43 (2) (2009) 319-328.
[7] N. Gao, J. Niu, Q. He, T. Zhu, J. Wu, Using RANS turbulence models and Lagrangian approach to predict particle deposition in turbulent channel flows. Build Environ. 48 (2012) 206-214.
[8] G. Lo Iacono, PG. Tucker, AM. Reynolds. Predictions for particle deposition from LES of ribbed channel flow. Int. J. Heat Fluid Flow 26 (4) (2005) 558-568.
[9] H. Lu, L. Lu, Numerical investigation on particle deposition enhancement in duct air flow by ribbed wall. Build Environ. 85 (2015a) 61-72.
[10] H. Lu, L. Lu, A numerical study of particle deposition in ribbed duct flow with different rib shapes. Build Environ. 94 (2015b) 43-53.
[11] H. Lu, L. Lu, Effects of rib spacing and height on particle deposition in ribbed duct air flows. Build Environ. 92 (2015c) 317-327.
[12] H. Lu, L. Lu, CFD investigation on particle deposition in aligned and staggered ribbed duct air flows. Appl. Therm. Eng. 93 (2016) 697-706.
[13] J. Kim, P. Moin, R. Moser. Turbulence statistics in fully developed channel flow at low Reynolds number. J Fluid Mech. 177 (1987) 133-166.
[14] FLUENT Inc. FLUENT 14.0 User's Guide, Lebanon, NH, 2011.
[15] EA. Matida, WH. Finlay, CF. Lange, B. Grgic, Improved numerical simulation of aerosol deposition in an idealized mouth–throat. J. Aerosol Sci. 35 (1) (2004) 1-19.